Yasemin Simsek Turker*[1]

Experimental Investigation of Rotational Behavior of Glulam Column-Beam Connection Reinforced with Carbon, Glass, Basalt and Aramid FRP Fabric

Eksperimentalno istraživanje rotacijskog ponašanja spoja između lameliranog stupa i grede ojačanoga polimernim tkaninama s vlaknima karbona, stakla, bazalta i aramida

ORIGINAL SCIENTIFIC PAPER
Izvorni znanstveni rad
Received – prispjelo: 20. 11. 2023.
Accepted – prihvaćeno: 31. 1. 2024.
UDK: 674.028; 674.06
https://doi.org/10.5552/drvind.2024.0162

ABSTRACT • *In the domain of modern timber structural systems, timber frame constructions distinguish themselves as preferred and commonly used building methods. Their appeal arises from their architectural adaptability and their distinctive attributes, which enable rapid assembly. In this type of structural system, the effectiveness of the connections between beams and columns plays a pivotal role in determining how forces are distributed, ensuring lateral stiffness, and upholding structural safety. Various methods have been developed to ensure column-beam connections in wooden structures. Column-beam connection points deteriorate and get damaged over time. These critical areas need to be strengthened over time. In this study, glulam columns (140 mm × 140 mm) and beams (140 mm × 280 mm), which are often used as load-bearing elements in wooden structures, were used. Columns and beams are connected to each other according to the wooden notching method. Column-beam connection areas are reinforced with carbon, glass, basalt and aramid fiber reinforced polymer fabrics. After the strengthening process, bending tests of the column-beam connection samples were carried out and the load carrying capacity, total amount of energy consumed, and maximum stiffness values were determined. Additionally, FRP damages occurring in the column-beam connection areas were observed during the experiments. The optimal outcomes for encasing column-beam connections have been identified with carbon-based fiber reinforced polymers. Glass-based fiber reinforced polymers yielded the least favorable results. Aramid-based fiber-reinforced polymers demonstrated similar outcomes to those wrapped with carbon-based counterparts. Consequently, it can be deduced that reinforcing column-beam connections with FRP fabrics, be they carbon, aramid, basalt, or glass-based, can markedly enhance their strength and durability, thereby extending their operational lifespan.*

KEYWORDS: *glulam, column-beam, connection, FRP fabric, reinforced*

* Corresponding author
[1] Author is researcher at Suleyman Demirel University, Faculty of Engineering, Department of Civil Engineering, Isparta, Turkey.

SAŽETAK • *U suvremenim konstrukcijama drvene se okvirne konstrukcije smatraju poželjnima i često su primjenjivane metode gradnje. Njihova prikladnost proizlazi iz njihove arhitektonske prilagodljivosti i prepoznatljivih svojstava koja omogućuju brzu montažu. U toj vrsti konstrukcijskog sustava učinkovitost spoja grede i stupa ima ključnu ulogu u određivanju načina raspodjele sila, osiguravanju bočne krutosti i održavanju strukturne sigurnosti. Razvijene su različite metode za osiguranje spojeva stupova i greda u drvenim konstrukcijama. Spojne točke stupova i greda s vremenom propadaju i oštećuju se, pa ih treba ojačati. U ovom su istraživanju korišteni lamelirani stupovi (140 mm × 140 mm) i lamelirane grede (140 mm × 280 mm) koje se često upotrebljavaju kao nosivi elementi u drvenim konstrukcijama. Stupovi i grede međusobno su povezani kutnim trokrakim spojem s pravokutnim urezima. Područja spoja grede i stupa ojačana su polimernim tkaninama ojačanim vlaknima karbona, stakla, bazalta i aramida. Nakon procesa ojačanja spoja provedena su ispitivanja na savijanje uzoraka spoja stupa i grede te su određene nosivost, ukupna količina utrošene energije i maksimalne vrijednosti krutosti. Osim toga, tijekom pokusa praćena su oštećenja polimernih tkanina ojačanih vlaknima koja su se dogodila u područjima spoja stupa i grede. Optimalni rezultati za ojačanje spojeva stupa i grede dobiveni su s polimernom tkaninom kojoj su dodana karbonska vlakna. Polimerna tkanina ojačana staklenim vlaknima dala je najnepovoljnije rezultate. Polimerne tkanine ojačane vlaknima na bazi aramida pokazale su slične rezultate kao i polimerne tkanine ojačane karbonskim vlaknima. Posljedično, može se zaključiti da ojačanje spojeva stupa i grede polimernim tkaninama kojima su dodana vlakna, bilo da je riječ o karbonu, aramidu, bazaltu ili staklu, može znatno povećati njihovu čvrstoću i izdržljivost, čime se produljuje njihov vijek trajanja.*

KLJUČNE RIJEČI: *lamelirano drvo; spoj stupa i grede; polimerne tkanine ojačane polimernim vlaknima; ojačanje*

1 INTRODUCTION
1. UVOD

Timber, as a widespread and natural resource, has been used for centuries in the building of housing and lightweight structures. The relatively recent development of laminated timber and other engineered wood products has further enabled timber to be used in buildings with a higher structural performance requirement, including long-span systems and mid- and high-rise building projects.

Over time, timber structures are vulnerable to biodegradation, including fungal, bacterial, and insect damage. These factors diminish their load-bearing capacity, necessitating frequent maintenance and restoration efforts (Li *et al*., 2017). Preserving ancient timber buildings requires a "heritage-respecting" approach, prioritizing their integrity and striving to restore them as faithfully as possible to their original state. This approach avoids extensive replacement of original building materials (Kilincarslan and Türker, 2020). Traditional restoration methods for timber structures, which impact their load-bearing properties and construction processes, are intricate and may result in additional structural harm. Modern technology allows for a more precise approach, addressing damaged sections individually and incorporating new materials for restoration in a scientifically sound manner (Borri *et al.*, 2013; Franke *et al.*, 2015; Gomez and Svecova, 2008; Hoseinpour *et al.*, 2018; Zhou *et al.*, 2015). Recent research and practical applications have demonstrated that Fiber Reinforced Polymer (FRP) has emerged as the leading technology for strengthening aging and deteriorating structures (Biscaia *et al.*, 2016; Kabir *et al.*, 2016; Vanerek *et al.*, 2014).

FRP composites have found extensive application in fortifying historical wooden edifices due to their lightweight nature, impressive strength, and resistance to corrosion (Athijayamani *et al.*, 2010; Ku *et al.*, 2011; Li *et al.*, 2014; Lopez-Anido *et al.*, 2005; Malkapuram *et al.*, 2009; Morales-Conde *et al.*, 2015; Valluzzi *et al.*, 2015). At present, there are two primary methods for reinforcing timber structures with FRP: (1) Near-Surface Mounted (NSM), involving the mechanical coupling of timber and composite plates, and (2) Externally Bonded Reinforcement (EBR), wherein composite plates are affixed to the outer surface of the timber (Rescalvo *et al.*, 2019). While NSM excels in terms of reinforcement strength (Isleyen *et al.*, 2021a), EBR technology boasts advantages such as simplified construction, reduced stress concentration, enhanced ductility, minimal aesthetic disruption, and widespread use in matrix reinforcement (İşleyen *et al.*, 2021b; Kilincarslan and Turker, 2021).

The exploration of glulam beams primarily revolves around enhancing wood resistance to bending and its overall strength. Presently, scholars worldwide have engaged in extensive investigations regarding the fortification of timber beams in two primary directions: the chemical alteration of wood or reinforcing substances and the physical enhancement of beams. This latter approach predominantly involves the incorporation of steel bars (Yang and Liu, 2006; Wei *et al.*, 2014), the affixation of steel plates (Yang, 2016), and the bonding of composite reinforcing materials (Zhou *et al.*, 2020; Gilbert *et al.*, 2014). Furthermore, research indicates that both methods effectively enhance the material properties of wood, with physical reinforcement notably exerting a more substantial influence on augmenting the load-bearing capacity of glulam beams, encompassing

flexural strength and stiffness. Presently, there is considerable interest in the performance of FRP materials when combined with other substances (Xiong *et al.*, 2022). The use of FRP for reinforcing flexural members is widespread, primarily owing to its exceptional tensile strength (Lu *et al.*, 2021; Dong *et al.*, 2019).

Among the array of composite reinforcement materials, carbon fiber-reinforced polymer (CFRP) stands out as the most widely used. In recent years, researchers have embarked on a series of empirical investigations concerning the augmentation of glulam beams through CFRP, delving into the intricacies of reinforcement mechanisms and failure modes (Yang and Sun, 2009; He *et al.*, 2022; Vahedian *et al.*, 2019). These endeavors have illuminated the profound capacity of CFRP to significantly enhance the load-bearing prowess of glulam beams, resulting in a ductile failure mode for the reinforced counterparts (Issa and Kmeid, 2005; Ma *et al.*, 2005). Furthermore, the research demonstrates that the incorporation of two and three layers of CFRP composite sheets results in remarkable increases in flexural strength, registering at 41.82 % and 60.24 %, respectively, when compared to their unreinforced timber counterparts (Khelifa *et al.*, 2015). Notably, CFRP also imparts heightened stiffness and elastic modulus to the beams.

Xie *et al*. (2007) and Wang *et al*. (2010) provided the calculation equations for ultimate bearing capacity and ultimate bending moment. Timbolmas *et al*. introduced an analytical model for forecasting the bending behavior of composite glulam beams under tension and compression, aligning their predictions with experimental results and demonstrating a minimal mean variation of around 15 %. Daniel *et al*. (2022) employed a probability design model and reliability analysis to assess CFRP-reinforced beams, the outcomes of which were rigorously confirmed through highly precise experiments. Moreover, widely used reinforcement materials encompass basalt fiber-reinforced polymer (BFRP) (Xiong *et al*., 2022), glass fiber-reinforced polymer (GFRP) (Todorovic *et al*., 2022), and natural fiber-reinforced polymer (NFRP). Wang *et al*., (2022), Zuo *et al*., (2015) and Wdowia and Brol (2019) conducted reinforcement of glulam beams using BFRP and subsequently scrutinized their structural performance, encompassing bearing capacity and deflection. This approach was deemed proficient in enhancing the bending resistance of glulam beams, thus mitigating the adverse impacts stemming from wood defects. Furthermore, Hay *et al*. (2006) validated the efficacy of a diagonal scheme in augmenting the average ultimate load, flexural stiffness, and deformability of the beams. Additionally, this study underscored the superiority of diagonal GFRP sheets over vertical sheets for shear-strengthening timber stringers.

Emerson (2004) undertook the reinforcement of deteriorated timber pier columns using glass fiber reinforced polymer (GFRP). His research demonstrated that the bearing capacity of GFRP-reinforced timber columns surpassed that of bare timber columns by approximately 17 %. Chidiaq (2003) conducted axial compression experiments on timber columns fortified with CFRP, revealing that the load-bearing capacity of these enhanced timber columns witnessed an augmentation of 15–25 %. Mallinath (2005) delved into experimental investigations involving glulam columns reinforced with both GFRP and CFRP. The findings indicated that CFRP exhibited a more pronounced strengthening effect compared to GFRP. Furthermore, Taheri (2005) embarked on a CFRP reinforcement study focusing on square glulam columns. His work demonstrated that the load-bearing capacity of the reinforced glulam columns experienced a substantial increase, ranging from approximately 60 % to 70 %.

Vetter *et al*. (2021) carried out an analytical investigation into how wood material properties impact the flexural behavior of FRP-reinforced glulam. This study encompassed an exploration of three distinct cross-sectional dimensions, two reinforcement techniques (simple tension and U-shaped reinforcement up to mid-depth), six varying quantities of FRP layers (ranging from 0 to 7), and three different ratios of tension-to-compression moduli (2:1, 1:1, 0.5:1), totaling 99 simulations. The ratio of tensile-to-compressive wood strength emerged as a pivotal factor influencing moment resistance enhancements, particularly when wood in tension exhibited significant weakness compared to compression (0.5:1), resulting in a substantial 1.95-fold moment resistance increase. Conversely, in cases where wood in tension outperformed that in compression (2:1), the maximum moment resistance increase observed was 1.19. This finding aligns with prior literature, emphasizing that FRP contribution is most pronounced for specimens with weaker wood properties (Johns and Lacroix, 2000).

In this study, the glulam column-beam connection, which is combined with a wood notching connection, is wrapped with 4 different fiber reinforced polymers: carbon, glass, basalt and aramid. After winding, the rotational behavior of the cone-beam connections under cyclic loads was investigated. As a result, load carrying capacity, total energy consumption and maximum stiffness values were examined.

2 MATERIALS AND METHODS
2. MATERIJALI I METODE

In this study, layered laminated timber columns and beams produced from spruce wood were used. 140 mm × 140 mm (C1414) column and 140 mm ×

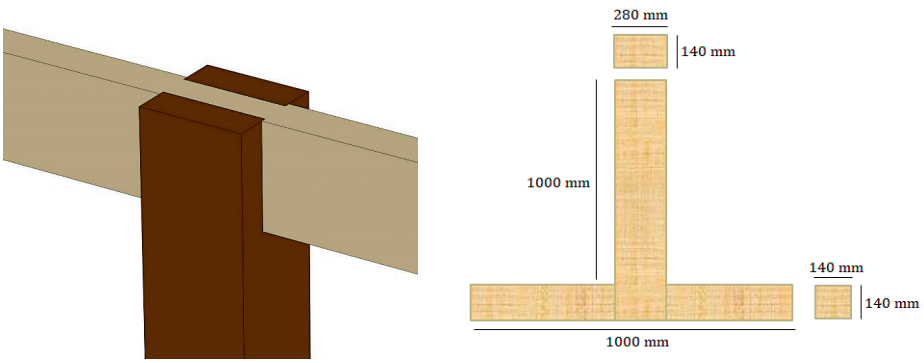

Figure 1 Wooden notched column-beam connection, A: Wooden notched connection example, B: Figural representation of dimensions of column-beam connection
Slika 1. Kutni trokraki spoj stupa i grede s pravokutnim urezima, A: primjer kutnog trokrakog spoja s pravokutnim urezima, B: shematski prikaz dimenzija spoja stupa i grede

280 (B1428) mm beam elements are connected to each other with a wooden notched connection. Columns and beams were supplied from Nasreddin Forest Products (Naswood) Antalya. By laminating spruce timbers with melamine formaldehyde glue and a balancing humidity of 11–12 %, glulam columns and beams are created. The columns and beams made of spruce glulam at the plant fall within the GL24h resistance class. Glulam beams have the features: 16.5 MPa tensile parallel, 0.5 MPa tensile rectangular, 24 MPa pressure parallel, 2.5 MPa shear and torsion, 11,600 MPa modulus of elasticity parallel, 390 MPa modulus of elasticity rectangular and 720 MPa shear modulus.

140 mm × 140 mm columns and 140 mm × 280 mm beams are connected to each other using wooden notched connections. The wood notch connection is given in Figure 1.

The FRP application was made with glass, carbon, aramid and basalt at the joints of the connected columns and beams. The properties of the column-beam connection samples to be tested are given in Table 1.

Figure 2 shows the image of the fiber reinforced polymer fabrics used in the study. The properties of the four fabrics are given in Table 2.

The strengthening process with fiber reinforced polymers was done in four stages. First, the application surfaces were cleaned so that the application could be carried out correctly and the FRPs could adhere. After cleaning the surfaces of wooden columns and beams, the primer was applied to the surfaces. After applying the primer, the surface was allowed to dry and then epoxy adhesive was applied to the surface. FRP fabrics (previously cut to the appropriate dimensions) were applied to the adhesive applied surfaces. In the final stage, epoxy adhesive was applied again on the FRP fabrics.

Carbon, glass, basalt and aramid-based fiber reinforced polymers were used in the study. The technical specifications of the fiber reinforced polymers used are available in UNAL TEKNIK catalogs (UNAL-

Table 1 Properties and codes of samples produced
Tablica 1. Svojstva i oznake pripremljenih uzoraka

No *Red. br.*	**Column size** *Dimenzije stupa,* mm	**Beam size** *Dimenzije grede,* mm	**Reinforcement fabric type** *Vrsta ojačanja tkanine*	**Reinforcement status** *Status ojačanja*	**Sample code** *Oznaka uzorka*
1	140x140	140x280	-	-	C1414B1428-UR
2	140x140	140x280	Glass	+	C1414B1428-G-R
3	140x140	140x280	Carbon	+	C1414B1428- C-R
4	140x140	140x280	Aramid	+	C1414B1428-A-R
5	140x140	140x280	Basalt	+	C1414B1428-B-R

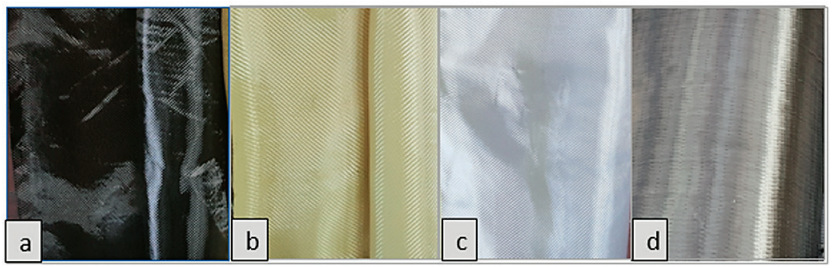

Figure 2 Fiber reinforced polymer fabrics: a) Basalt based FRP, b) Aramid based FRP, c) Glass based FRP, d) Carbon based FRP
Slika 2. Polimerne tkanine ojačane vlaknima: a) na bazi bazalta, b) na bazi aramida, c) na bazi stakla, d) na bazi karbona

Table 2 Properties of carbon, glass, aramid and basalt fabrics
Tablica 2. Svojstva karbonskih, staklenih, aramidnih i bazaltnih tkanina

Material properties *Svojstva materijala*	**Carbon** *Karbon*	**Aramid**	**Glass** *Staklo*	**Basalt** *Bazalt*
Weight / *gramaža,* g/m^2	300	300	300	200
Modulus of elasticity, GPa / *modul elastičnosti,* GPa	230	100	72	82
Tensile strength, N/mm^2 / *vlačna čvrstoća,* N/mm^2	4900	3300	3900	3200
Design section thickness, mm / *dizajnirana debljina presjeka,* mm	0.166	0.170	0.162	0.167

Figure 3 Strengthening stage with fiber reinforcement polymer fabrics
Slika 3. Faza ojačanja polimernim tkaninama s dodanim vlaknima

TEKNIK, 2023). Strengthening of column-beam connection areas was done in 5 stages. First, the rear part of the column was strengthened, and then the beam was wrapped. Then, the column and beam connection points were strengthened at a 45-degree angle. Finally, the upper and lower parts of the arm were reinforced in the connection area. The strengthening phase of column-beam connection areas is given in Figure 4.

The reinforcement steps given in Figure 4 were performed for four different fiber-reinforced polymers. The load-displacement test was carried out in a sufficiently strong frame created with steel bearing elements. The experimental setup is given in Figure 5.

During the experiments, the specimens underwent multiple cycles of controlled displacements applied at the beam end positions. The loading speed was set to 0.2 mm/s. Figure 6 illustrates the sequence of loading stages employed in every test, totaling 24 steps (with each step repeated three times).

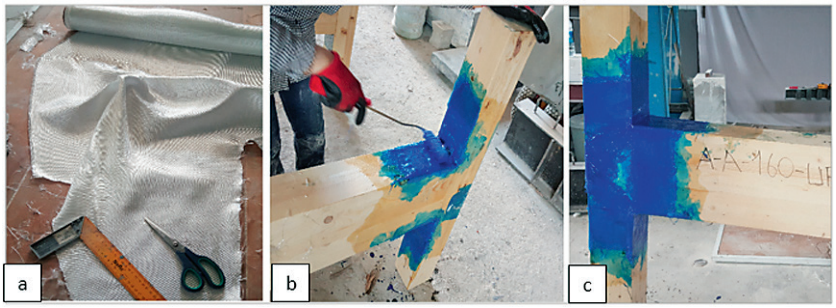

Figure 4 Strengthening phase: a) Sizing of FRP fabrics, b) Application of FRP fabrics, c) Final state of column-beam connection wrapped with FRP
Slika 4. Faze ojačanja: a) dimenzioniranje FRP tkanina, b) primjena FRP tkanina, c) konačno stanje spoja stupa i grede omotane FRP-om

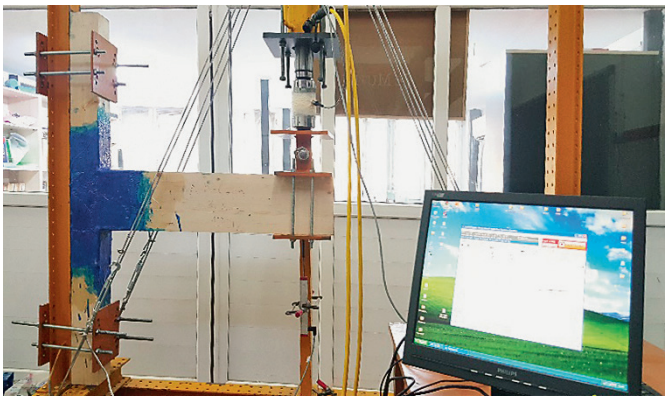

Figure 5 Experimental setup installed in the laboratory
Slika 5. Postavka eksperimenta u laboratoriju

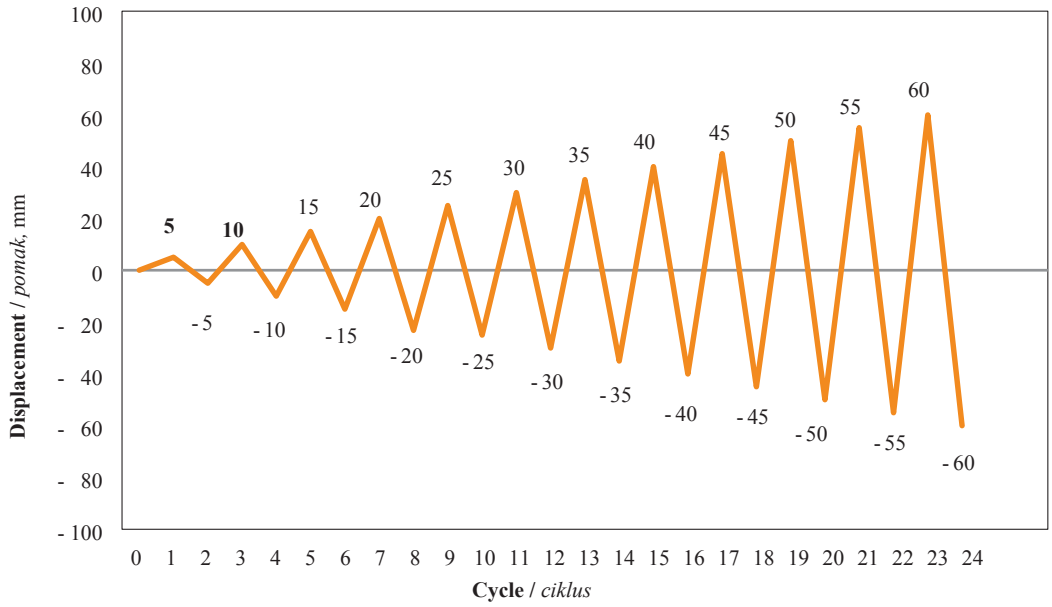

Figure 6 Basic loading steps for all experiments
Slika 6. Osnovni koraci opterećenja za sve eksperimente

The specimens experienced cyclic vertical displacements in both the upward and downward directions. Analyzing the load-displacement graphs provided insights into the structural responses of the materials investigated in these studies.

The assessment focused on the samples ability to dissipate energy and on how their stiffness evolved during the trial. Load-displacement graphs obtained at the end of each experiment were instrumental in the calculations. These graphs were initially segregated into cycles for each sample. The push and pull directions of each cycle were used to compute the stiffness values (k) of the samples. In these computations, the stiffness values were derived by determining the gradient of the line connecting the load points corresponding to the most significant displacements in the push and pull directions with the load positions where the load transitions sign. The connection stiffness Kj for each degree of loading displacement was computed as (Zhang *et al.*, 2020).

$$K_J = \frac{\sum_{i=1}^{n} F_J^i}{\sum_{i=1}^{n} D_j^i} \tag{1}$$

At the occurrence of the i^{th} cycle at the j^{th} level of loading displacement, the peak load is denoted as F_J^i and the corresponding displacement as D_j^i.

Through the calculation of the enclosed areas beneath the load-displacement curves for each cycle within the samples, the capacity of the samples for dissipating energy was assessed. The cumulative sum of these areas at the end of the experiment reflects the overall energy dissipation capability of the sample. Additionally, the hysteresis curve provides a means to ascertain the equivalent viscous damper ratio, a pivotal metric in quantifying energy dissipation capacity (Zhang *et al.*, 2020; Sasmal *et al.*, 2011).

$$E = \frac{S(ABC + CDA)}{S(OBE + ODF)'} \tag{2}$$

$$\zeta_{eq} = \frac{1}{2\Pi} \cdot \frac{S\left(ABC + CDA\right)}{S\left(OBE + ODF\right)'} \tag{3}$$

Let S (ABC + CDA) denote the hysteresis loop area, while S (OBE + ODF) represents the combined area of triangles OBE and ODF. In this context, E stands for the energy dissipation coefficient. The parameter ζeq, known as the equivalent viscous damper ratio, is determined by the ratio of the energy dissipated within the hysteretic loop to the strain energy, divided by the constant 2π.

The estimation of plastic deformation energy absorbed by the sample is derived from the energy dissipation capacity using the methods outlined in (Chopra, 1995). These computations unveiled the sample capacity for energy dissipation in each cycle, as well as the total energy dissipated by the conclusion of the experiment. Additionally, each cycle encompassed the assessment of the sample stiffness values in both push and pull directions.

3 RESULTS AND DISCUSSION
3. REZULTATI I RASPRAVA

3.1 Load-Displacement
3.1. Graf opterećenje – pomak

Figure 7 presents the load-displacement graph for sample code C1414B1428-UR, C1414B1428-G-R,

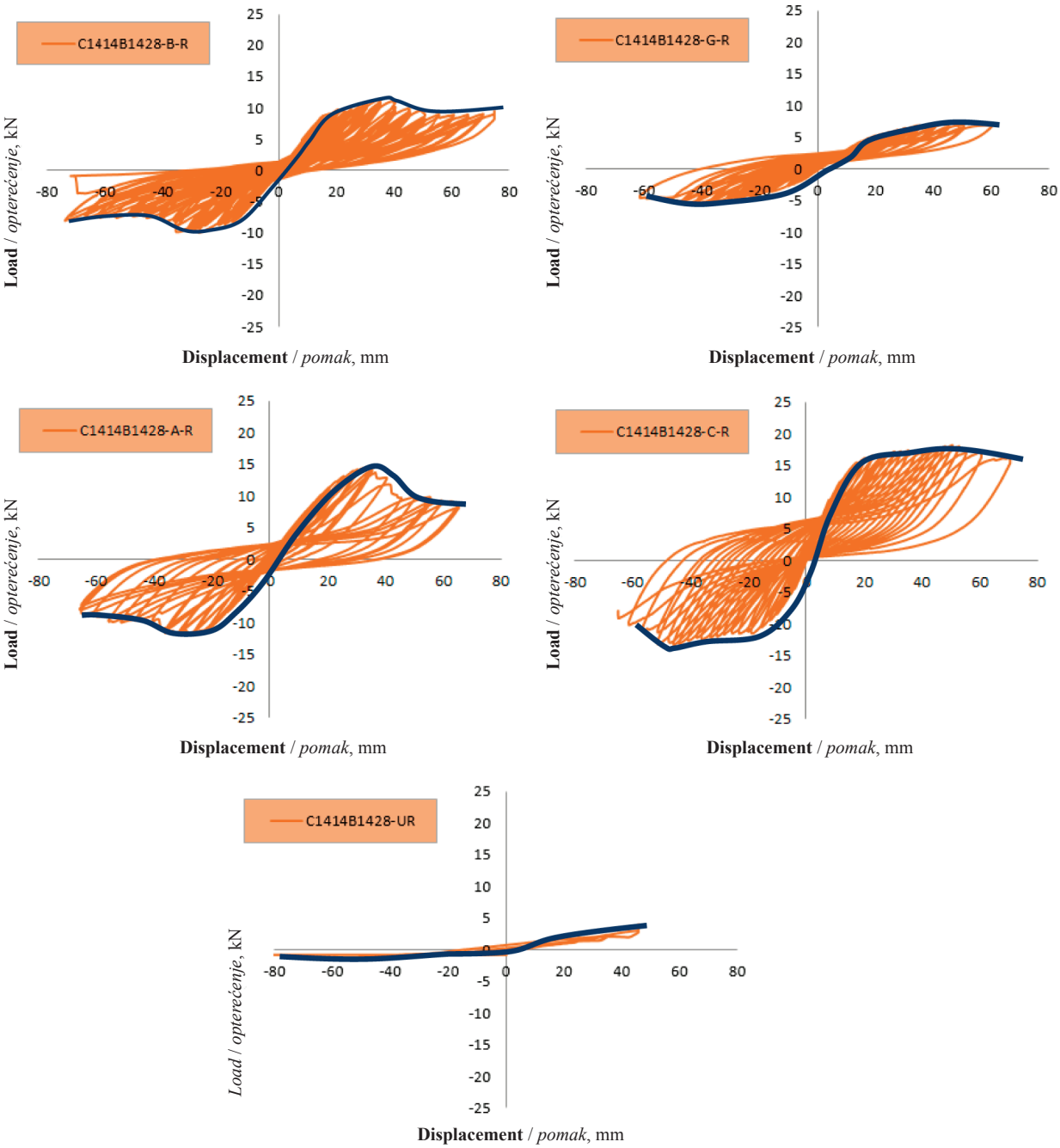

Figure 7 Load-displacement graph of S1212K1224-G-UR, S1212K1224-1-G-R, S1212K1224-2-G-R, and S1212K1224-3-G-R column-beam samples
Slika 7. Graf opterećenje – pomak za uzorke spoja stupa i grede S1212K1224-G-UR, S1212K1224-1-G-R, S1212K1224-2-G-R te S1212K1224-3-G-R

C1414B1428-C-R, C1414B1428-B-R, and C1414B1428-A-R.

The unreinforced sample labeled as C1414K1428-UR demonstrated a peak load-bearing capacity of 6.37 kN during the push (positive) phase and 8.79 kN during the pull (negative) phase. Analyzing the results of the reinforced samples, C1414K1428-C-R displayed load-bearing capacity of 17.64 kN in the push direction and 15.48 kN in the pull direction. For the C1414K1428-A-R sample, the load-bearing capacity was measured at 14.18 kN in the push direction and 13.27 kN in the pull direction. The C1414K1428-B-R sample exhibited load-bearing capacity of 12.10 kN in the push direction and 10.07 kN in the pull direction. For the C1414K1428-G-R sample, the load-bearing capacity was measured at 08.21 kN in the push direction and 06.72 kN in the pull direction. Furthermore, a comparison of strength reduction was conducted between the cycle where each sample reached its load-bearing capacity and the most recent cycle. When the load carry-

ing capacity values were examined, it was determined that the highest load carrying capacity was obtained in the column-beam connection wrapped with carbon-based fiber reinforced polymers. It was determined that the load carrying capacity of the column-beam connection wrapped with carbon-based fiber-reinforced polymer was approximately 128.57 % higher than the column-beam connection wrapped with glass-based fiber-reinforced polymer.

3.2 Energy dissipation capacities
3.2. Kapaciteti rasipanja energije

The calculation of energy dissipation capacity in the specimens involved determining the enclosed areas under the load-displacement curves throughout each cycle. Primarily, a comprehensive comparison of energy dissipation capacity was performed across all the samples. Figure 8 shows the total energy dissipation consumed (*TEDC*) and the cycle energy dissipation capacity (*CEDC*) values of the column-beam connections reinforced 1, 2 and 3 times with carbon fiber reinforced polymer. Figure 8 shows the total energy consumption (*TEDC*) and cycle energy dissipation capacity (*CEDC*) values of column-beam connections reinforced with carbon, glass, basalt and aramid-based fiber-reinforced polymer.

It was determined that the highest energy absorption capacity value belongs to the C1414B1428-C-R sample reinforced with 2526 kN·mm, while the lowest value belongs to the C1414B1428-UR sample reinforced with 2111 kN·mm. Among the wrapped column-beam connections, the energy consumption capacity of the column-beam connections wrapped with glass fiber reinforced polymers had the lowest value. This highlights the notable effectiveness of the FRP retrofitting approach in this context.

Upon examination of Figure 9, it becomes evident that the stiffness values of the sample C1414B1428-C-R surpass those of the other samples in both directions, namely the push and pull (maximum stiffness value in the push direction: 984 kN/m, maximum stiffness value in the pull direction: 997 kN/m). Conversely, the samples with the sample code C1414B1428-UR exhibit the lowest stiffness values in both directions (maximum stiffness in the push direction: 610 kN/m, maximum stiffness in the pull direction: 611 kN/m). In wrapped column-beam connections, the stiffness value of the C1414B1428-C-R sample connection is approximately 38 % higher than the C1414B1428-G-R sample connection, 24 % higher than the C1414B1428-B-R sample connection, and 18 % higher than the C1414B1428-A-R sample connection. This result is

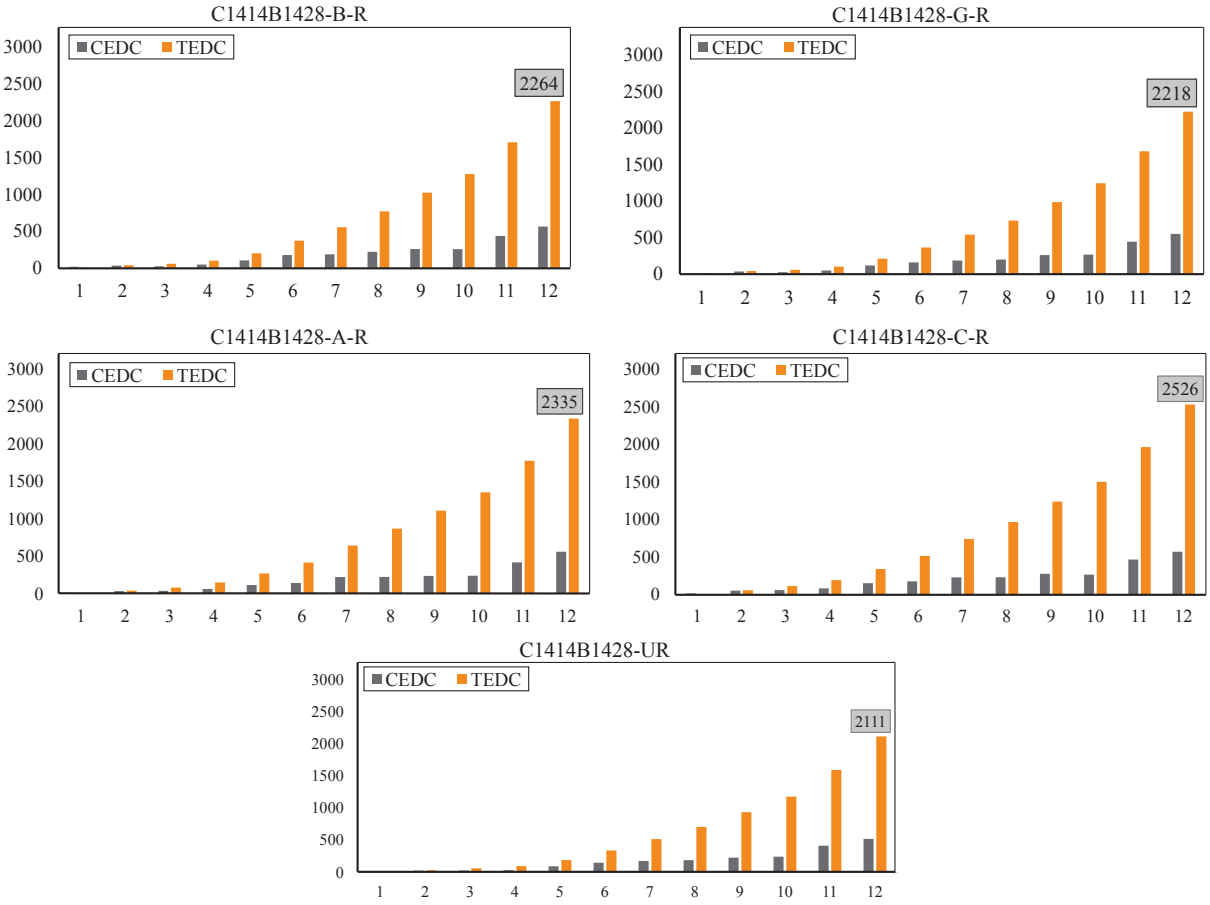

Figure 8 Energy consumption capacities of column-beam connections reinforced with carbon, glass, basalt and aramid
Slika 8. Kapaciteti potrošnje energije spojeva stupa i grede ojačanih karbonom, staklom, bazaltom i aramidom

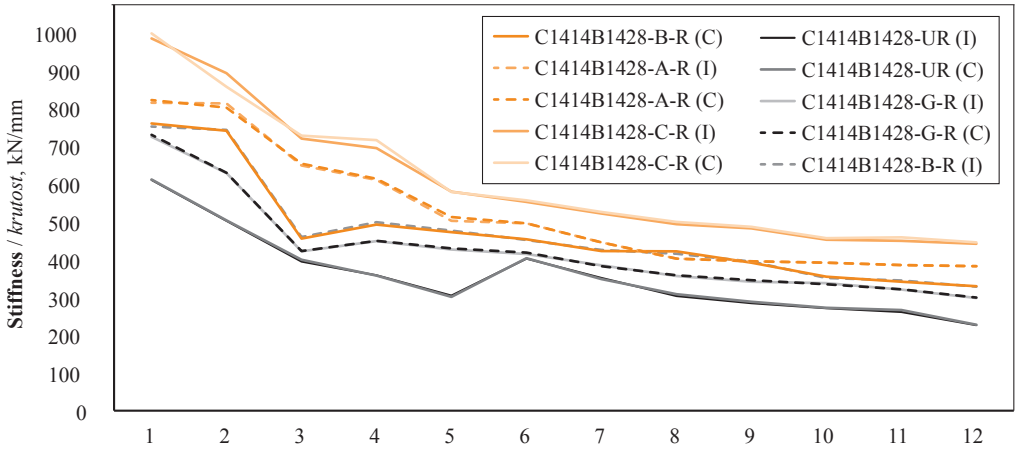

Figure 9 Change in stiffness in push (I) and pull (C) direction of samples reinforced with carbon, aramid, basalt, glass fiber polimers
Slika 9. Promjena krutosti u smjeru guranja (I) i povlačenja (C) uzoraka ojačanih ugljičnim, aramidnim, bazaltnim i staklenim vlaknima

consistent with the investigation carried out by Mangır (2018) and Kılıncarslan and Simsek Turker (2021), who examined the rotational performance of concrete column-beam assemblies. In their research, Mangır (2018) and Kılıncarslan and Simsek Turker (2021), observed that the rigidity measurements of the samples reinforced with FRP surpassed those of the unreinforced sample. In all samples, the initial rigidity progressively diminished in both orientations over the course of the experiment owing to the formation of cracks and ruptures in the FRP material.

3.3 FRP Damages in joint zones during the experiment
3.3. Oštećenja polimernih tkanina ojačanih vlaknima u zonama spoja tijekom eksperimenta

In this study, wrapping was carried out in the column-beam regions with four types of fiber-reinforced polymer fabrics. As a result of the wrapping, experiments were carried out on the column-beam connection samples. During the experiments, images of fractures and explosions occurring in carbon, aramid, basalt and glass fiber reinforced polymers were recorded. A few of the images obtained during the study are given in Figure 10.

4 CONCLUSIONS
4. ZAKLJUČAK

In this study, the glulam column-beam connection, which is combined with a wood notching connection, is wrapped with four different fiber reinforced polymers: carbon, glass, basalt and aramid. After winding, the rotational behavior of the cone-beam connections under cyclic loads was investigated. As a result, the values of the load carrying capacity, total energy consumption and maximum stiffness were examined.

When the load carrying capacity values were examined, it was determined that the highest load carrying capacity was obtained in the column-beam connection wrapped with carbon-based fiber reinforced polymers. It was determined that the load carrying capacity of the column-beam connection wrapped with carbon-based fiber-reinforced polymer was approxi-

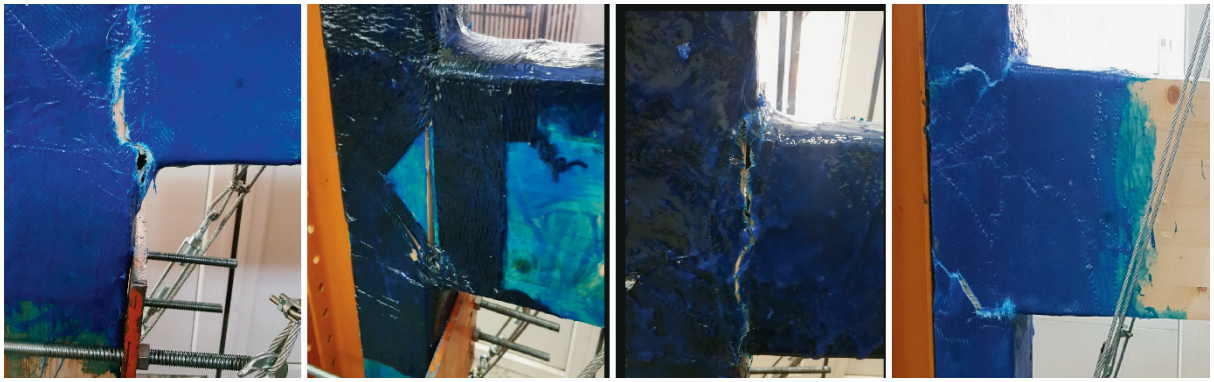

a) b) c) d)

Figure 10 FRP damages in joint zones during the experiment: a) Aramid, b) Carbon, c) Basalt, d) Glass FRP
Slika 10. Oštećenja polimernih tkanina ojačanih vlaknima u zonama spoja tijekom eksperimenta: a) aramid, b) karbon, c) bazalt, d) staklo

mately 128.57 % higher than the column-beam connection wrapped with glass-based fiber-reinforced polymer.

It was determined that the highest energy absorption capacity belongs to the C1414B1428-C-R sample reinforced with 2526 kN.mm, while the lowest value belongs to the sample C1414B1428-UR reinforced with 2111 kN.mm. Among the wrapped column-beam connections, the energy consumption capacity of the column-beam connections wrapped with glass fiber reinforced polymers had the lowest value. This highlights the notable effectiveness of the FRP retrofitting approach in this context. In wrapped column-beam connections, the stiffness value of the C1414B1428-C-R sample connection is approximately 38 % higher than the C1414B1428-G-R sample connection, 24 % higher than the C1414B1428-B-R sample connection, and 18 % higher than the C1414B1428-A-R sample connection.

In summary, it has been verified that the reinforced samples exhibit higher stiffness values compared to the unreinforced ones. Furthermore, the incorporation of column-beam combinations in all samples has resulted in elevated load-carrying capacities, enhanced levels of energy dissipation, and improved stiffness. It has been determined that the best results in wrapping column-beam connections are obtained with carbon-based fiber reinforced polymers. It has also been determined that the lowest values were obtained with glass-based fiber reinforced polymers. It has been determined that column-beam connections wrapped with aramid-based fiber-reinforced polymers give similar results to connections wrapped with carbon-based fiber-reinforced polymers. As a result, it can be concluded that the strength and durability of column-beam connections reinforced with carbon, aramid, basalt and glass-based FRP fabrics can be significantly increased and thus their service life can be extended.

5 REFERENCES
5. LITERATURA

1. Athijayamani, A.; Thiruchitrambalam, M.; Manikandan, V.; Pazhanivel, B., 2010: Mechanical properties of natural fibers reinforced polyester hybrid composite. International Journal of Plastics Technology, 14 (1):104-116. https://doi.org/10.1007/ s12588-009-0016-0
2. Biscaia, H. C.; Chastre, C.; Borba, I. S.; Silva, C.; Cruz, D., 2016: Experimental evaluation of bonding between CFRP laminates and different structural materials. Journal of Composites for Construction, 20 (3). https://doi.org/10.1061/(ASCE)CC.1943-5614.0000631
3. Borri, A.; Corradi, M.; Speranzini, E., 2013: Reinforcement of wood with natural fibers. Composites. Part B: Engineering, 53:1-8. https://doi.org/10.1016/j.compositesb.2013.04.039
4. Chidiaq, R., 2003: Axial compression of rounded wood poles reinforced with carbon fiber. MSc Special Project, Department of Civil Engineering, Rutgers, State University of New Jersey, Piscataway, N.J.
5. Chopra, A. K., 1995: Dynamics of structures: theory and applications to earthquake engineering. Prentice Hall, Englewood Cliffs, New Jersey.
6. Daniel, H.; Habashneh, M.; Rad, M. M., 2022: Reliability-based numerical analysis of glulam beams reinforced by CFRP plate. Scientific Reports, 12 (1): 13587.
7. Dong, Z. Q.; Wu, G.; Zhao, X. L.; Zhu, H.; Shao, X. X., 2019: Behaviors of hybrid beams composed of seawater sea-sand concrete (SWSSC) and a prefabricated UHPC shell reinforced with FRP bars. Construction and Building Materials, 213: 32-42. https://doi.org/10.1016/j.conbuildmat.2019.04.059
8. Emerson, R. N., 2004: In situ repair technique for decayed timber piles. Strutures Congress, 1:1-9.
9. Franke, S.; Franke, B.; Harte, A. M., 2015: Failure modes and reinforcement techniques for timber beams – State of the art. Construction and Building Materials, 97: 2-13. https://doi.org/10.1016/j.conbuildmat.2015.06.021
10. Gilbert, B. P.; Underhill, I. D.; Bailleres, H.; El Hanandeh, A.; McGavin, R. L., 2014: Veneer Based Composite hollow utility poles manufactured from hardwood plantation thinned trees. Construction and Building Materials, 66: 458-466. https://doi.org/10.1016/j. conbuildmat.2014.05.093
11. Gomez, S.; Svecova, D., 2008: Behavior of split timber stringers reinforced with external GFRP sheets. Journal of Composites for Construction, 12 (2): 202-211. https://doi.org/10.1061/(ASCE)1090-0268(2008)12:2(202)
12. Hay, S.; Thiessen, K.; Svecova, D.; Bakht, B., 2006: Effectiveness of GFRP sheets for shear strengthening of timber. Journal of Composites for Construction, 10 (6): 483-491. https://doi.org/ 10.1061/(ASCE)1090-0268(2006)10:6(483)
13. He, M. J.; Wang, Y. X.; Li, Z.; Zhou, L. A.; Tong, Y. C.; Sun, X. F., 2022: An experimental and analytical study on the bending performance of CFRP-reinforced glulam beams. Frontiers in Materials, 8: 802249. https://doi.org/10.3389/fmats.2021.802249
14. Hoseinpour, H.; Valluzzi, M. R.; Garbin, E.; Panizza, M., 2018: Analytical investigation of timber beams strengthened with composite materials. Construction and Building Materials, 191: 1242-1251. https://doi.org/10.1016/j.conbuildmat.2018.10.014
15. Isleyen, U. K.; Ghoroubi, R.; Mercimek, O.; Anil, O.; Erdem, R. T., 2021a: Behavior of glulam timber beam strengthened with carbon fiber reinforced polymer strip for flexural loading. Journal of Reinforced Plastics and Composites, 40 (17-18): 665-685. https://doi.org/10.1177/ 0731684421997924
16. İşleyen, Ü. K.; Ghoroubi, R.; Mercimek, Ö.; Anil, Ö.; Togay, A.; Erdem, R. T., 2021b: Effect of anchorage number and CFRP strips length on behavior of strengthened glulam timber beam for flexural loading. Advances in Structural Engineering, 24 (9): 1869-1882. https://doi.org/10.1177/1369433220988622
17. Issa, C. A.; Kmeid, Z., 2005: Advanced wood engineering: glulam beams. Construction and Building Materials, 19 (2): 99-106. https://doi.org/10.1016/j.conbuildmat.2004.05.013
18. Johns, K. C.; Lacroix, S., 2000: Composite reinforcement of timber in bending. Canadian Journal of Civil Engineering, 27: 899-906.
19. Kabir, M. I.; Shrestha, R.; Samali, B., 2016: Effects of applied environmental conditions on the pull-out

strengths of CFRP-concrete bond. Construction and Building Materials, 114: 817-830. https://doi.org/10.1016/j.conbuildmat.2016.03. 195
20. Khelifa, M.; Auchet, S.; Meausoone, P. J.; Celzard, A., 2015: Finite element analysis of flexural strengthening of timber beams with Carbon Fibre-Reinforced Polymers. Engineering Structures, 101: 364-375. https://doi.org/10.1016/j.engstruct.2015.07.046
21. Kilincarslan, E.; Türker, Y., 2020: Investigation of wooden beam behaviors reinforced with fiber reinforced polymers. Organic Polymer Material Research, 2 (1): 7. https://doi.org/10.30564/opmr.v2i1.1783
22. Kilincarslan, S.; Turker, Y. S., 2021: Experimental investigation of the rotational behaviour of glulam column-beam joints reinforced with fiber reinforced polymer composites. Composite Structures, 262 (1): 113612. https://doi.org/10.1016/j. compstruct.2021.113612
23. Ku, H.; Wang, H.; Pattarachaiyakoop, N.; Trada, M., 2011: A review on the tensile properties of natural fiber reinforced polymer composites. Composites. Part B, 42 (4): 856-873. https://doi.org/10.1016/j.compositesb.2011.01.010
24. Li, J.; Zhang, X.; Li, J.; Li, R.; Qian, M.; Song, P., 2017: An experimental study of the damage degrees to ancient building timber caused by lightning strikes. Journal of Electrostatics, 90: 23-30. https://doi.org/10.1016/j.elstat.2017.08.009
25. Li, Y.; Tsai, M.; Wei, T.; Wang, W., 2014: A study on wood beams strengthened by FRP composite materials. Construction and Building Materials, 62: 118-125. https://doi.org/10.1016/j.conbuildmat.2014.03.036
26. Lopez-Anido, R. A.; Muszynski, L.; Gardner, D. J.; Goodell, B.; Herzog, B., 2005: Performance-based material evaluation of reinforced glued laminated timber (Glulam) beams. Journal of Testing and Evaluation, 33: 6.
27. Lu, Z.; Li, J.; Xie, J.; Huang, P.; Xue, L., 2021: Durability of flexurally strengthened RC beams with prestressed CFRP sheet under wet-dry cycling in a chloride-containing environment. Composite Structures, 255: 112869. https://doi.org/10.1016/j.compstruct.2020.112869
28. Ma, J. X.; Jiang, X. M.; Hu, P.; Hu, M., 2005: Experimental study on bending behaviour of timber beams reinforced with CFRP sheets. Industrial Construction, 35 (8): 35-39.
29. Malkapuram, R.; Kumar, V.; Negi, Y. S., 2009: Recent development in natural fiber reinforced Polypropylene composites. Journal of Reinforced Plastics and Composites, 28 (10): 1169-1189. https://doi.org/10.1177/0731684407087759
30. Mallinath, N., 2005: Experimental and computational investigation of FRP reinforced GLULAM columns including associated software development. Cananda: Dalhousie University.
31. Mangır, A., 2018: Experimental investigation on the seismic performance of beam-column joints in low-strength reinforced concrete structures. PhD Thesis, Istanbul University, Institute of Graduate Studies in Science and Engineering, İstanbul, Turkey.
32. Morales-Conde, M. J.; Rodriguez-Linan, C.; Rubio-De Hita, P., 2015: Bending and shear reinforcements for timber beams using GFRP plates. Construction and Building Materials, 96: 461-472. https://doi.org/10.1016/j.conbuildmat.2015.07.079
33. Rescalvo, F. J.; Suarez, E.; Abarkane, C.; Cruz-Valdivieso, A.; Gallego, A., 2019: Experimental validation of a CFRP laminated/fabric hybrid layout for retrofitting and repairing timber beams. Mechanics of Advanced Materials and Structures, 26 (22):1902-1909. https://doi.org/10.1080/15376494.2018.1455940
34. Sasmal, S.; Novák, B.; Ramanjaneyulu, K., 2011: Numerical analysis of fiber composite-steel plate upgraded beam-column sub-assemblages under cyclic loading. Composite Structures, 93 (2): 599-610. https://doi.org/10.1016/j.compstruct.2010.08.019
35. Taheri, F.; Nagaraj, M.; Cheraghi, N., 2005: FRP-Reinforced Glulaminated Columns. FRP International, 2 (3): 10-12.
36. Todorovic, M.; Glisovic, I.; Stevanovic, B., 2022: Experimental investigation of end-notched glulam beams reinforced with GFRP bars. European Journal of Wood and Wood Products, 80 (5): 10711085. https://doi.org/10.1007/s00107-022-01822-6
37. Vahedian, A.; Shrestha, R.; Crews, K., 2019: Experimental and analytical investigation on CFRP strengthened glulam laminated timber beams: full-scale experiments. Composites. Part B: Engineering, 164: 377-389. https://doi.org/10.1016/j. compositesb.2018.12.007
38. Valluzzi, M. R.; Nardon, F.; Garbin, E.; Panizza, M., 2015: Multi-scale characterization of moisture and thermal cycle effects on composite-to-timber strengthening. Construction and Building Materials, 102: 102. https://doi.org/10.1016/j.conbuild mat.2015.07.008
39. Vanerek, J.; Benesova, A.; Rovnanik, P.; Drochytka, R., 2014: Evaluation of FRP/wood adhesively bonded epoxy joints on environmental exposures. Journal of Adhesion Science and Technology, 28 (14-15):1405-1417. https://doi.org/10.1080/01694243. 2012.698096
40. Vetter, Y.; Stakheiko, M.; Chen, H.; Siciliano, S.; Lacroix, D., 2021: Analytical Investigation of Wood Material Properties on the Flexural Behaviour of FRP Reinforced Glulam. In: Proceedings of CSCE 2021 Annual Conference, pp. 10.
41. Wang, Q. F.; Li, F.; Chen, H. J.; Huang, Y. H.; Yang, Y. X., 2010: Experimental study on flexural behaviour of timber beams reinforced with BFRP sheets. Industrial Construction, 40 (4): 126-130.
42. Wang, Y. Z.; Ma, Y. P.; Wang, L. Q.; Li, F. T., 2022: Flexural behaviour of fast-growing poplar glulam beams reinforced by carbon fibre. Journal of Civil and Environmental Engineering, 44 (6): 124-135.
43. Wdowiak, A.; Brol, J., 2019: Effectiveness of reinforcing bent non-uniform pre-stressed glulam beams with Basalt Fibre Reinforced Polymers rods. Materials, 12: 3141. https://doi.org/10.3390/ma12193141
44. Wei, Y.; Wang, X. W.; Li, G. F., 2014: Mechanical properties test of bamboo scimber flexural specimens of reinforced with bars. Acta Materiae Compositae Sinica, 31 (4): 1030-1036.
45. Xie, Q. F.; Zhao, H. T.; Xue, J. Y.; Wu, Z. H., 2007: Experimental study on flexural performance of wood beams strengthened with CFRP sheets. Industrial Construction, 37 (7): 104-107.
46. Xiong, Z.; Lin, L H.; Qiao, S. H.; Li, LJ.; Li, Y. L.; He, S.; Li, Z.; Liu, F.; Yulong Chen, Y., 2022: Axial performance of seawater sea-sand concrete columns reinforced with basalt fibre-reinforced polymer bars under concentric compressive load. Journal of Building Engineering, 47: 103828. https://doi.org/10.1016/j.jobe.2021.103828
47. Xiong, Z.; Mai, G. H.; Chen, P. X.; Zeng, H. M.; Li, LJ.; Liu, F.; You, W. T., 2022: Investigation on fatigue bond behaviour between GFRP bars and seawater sea-sand

concrete. China Journal of Highway and Transport, 35 (2): 259-268.
48. Yang, H. F.; Liu, W. Q., 2006: Analysis study of flexural deformation of FRP reinforced glulam beams. Journal of Nanjing University of Technology, 6 (3): 1-5 + 14.
49. Yang, X. H., 2016: Research on the flexural behavior and design method for steel plate strengthened glulam beam. Harbin: Northeast Forestry University.
50. Yang, X. J.; Sun, Y. F., 2009: Study on flexural properties of glulam with reinforced carbon fibre. Forestry and Grassland Machinery, 10: 17-19 + 22.
51. Zhang, J.; Hu, X.; Sun, Q.; Zhang, Y.; Zhu, W.; Li, L., 2020: Experimental study on seismic performance of glulam-concrete composite beam-to-column joints. Composite Structures, 236: 111864. https://doi.org/10.1016/j.compstruct.2020.111864
52. Zhou, A.; Tam, L.-H.; Yu, Z.; Lau, D., 2015: Effect of moisture on the mechanical properties of CFRP-wood composite: An experimental and atomistic investigation. Composites. Part B: Engineering, 71: 63-73. https://doi.org/10.1016/j. compositesb.2014.10.051
53. Zhou, C. D.; Yang, L. G.; Shiha, A., 2020: Experimental study on flexural behaviour of timber beams strengthened in both tension and compression zone. China Civil Engineering Journal, 53 (11): 55-63. https://doi.org/10.15951/j.tmgcxb.2020.11.006
54. Zuo, H. L.; Bu, D. W.; Guo, N.; He, D. P., 2015: Effect of basalt fibre composite on flexural behaviour of gluam beams. Journal of Northeast Agricultural University, 43 (04): 91-95.
55. ***UNALTEKNIK, 2023: (online), http://unalteknikas.com.tr/ (Accessed Oct. 10, 2023).

Corresponding address:

YASEMIN SIMSEK TURKER
Suleyman Demirel University, Faculty of Engineering, Department of Civil Engineering, Isparta, TURKEY,
e-mail: yaseminturker@sdu.edu.tr